

Debuncher Beam Loading Considerations and New Parameters

LU — 160

James A. MacLachlan

11 June 90

Abstract

The momentum width of the 400 MeV beam from the linac is about 0.4 %; by using an 805 MHz debunching rf section about 40 m downstream of the linac it is possible in principle to reduce this by an order of magnitude at the booster. Practically, although such ideal debunching is not needed, care is still required to maintain the correct debuncher phase under transient beam loading. This note reviews the underlying design concepts and presents appropriate hardware parameters. It is suggested that a short DAW section may be a particularly good structure for the debuncher.

Distribution:

- T. Jurgens
- Q. Kerns
- T. Kroc
- G. Lee
- J. MacLachlan
- M. May
- H. Miller
- R. Noble
- L. Oleksiuk
- D. Young

Introduction

The beam bunches exiting the 400 MeV linac have about 12° full width and full momentum spread of 0.4%. The momentum spread would increase by about one third in transport to the booster at the 50 mA design intensity. No clear criterion has been set for the optimum momentum spread for booster injection, but one can frame a plausible requirement by working back from the smallest longitudinal emittance that one hopes to attain for intense booster bunches. In order not to preclude future miracles, plan for 0.02 eVs bunches at 5×10^{12} in the booster, *i.e.*, at 6×10^{10} protons per bunch. The debunched linac beam should then be something less than $84 \times 0.02 = 1.68$ eVs. The beam circulation period in the booster at 400 MeV is $2.218 \mu\text{s}$; therefore the energy spread should be limited by

$$\Delta E < \frac{hS_{\text{bnch}}}{\tau_{\text{circ}}} = 0.7574 \text{ MeV}$$

or

$$\frac{\Delta p}{p} = \frac{\Delta E}{\beta^2 E} < 0.113 \text{ \%}.$$

A full momentum spread at booster injection of 0.1 % therefore looks like a reasonable design criterion. This is nearly an order of magnitude broader than ideal debunching, but there seems no cause to struggle for the ultimate from the debuncher when there is no possibility for the booster to maintain a lower momentum spread at useful intensity. Even for this more practicable design goal, the design beam current is enough to require some care in controlling time dependence of the central energy and energy spread resulting from beam-induced shift of the debuncher phase.

The basic scheme for the debuncher is to drift the beam from the linac far enough that the bunches have spread to cover something in the range $60^\circ - 90^\circ$ of 805 MHz phase with strong correlation between phase and energy. After the drift the bunches pass through a cavity phased so that the leading particles are decelerated and trailing particles are accelerated closer to the central momentum. By neglecting the space charge forces one can estimate the required drift and cavity voltage from the initial energy spread. The spreading per unit drift length is given directly by the velocity spread:

$$\frac{\Delta s}{s} = \frac{\Delta \beta}{\beta}.$$

Replacing Δs by $\beta \lambda \Delta \varphi / 2\pi$ leads to

$$s = \frac{(\beta \gamma)^3 \lambda \Delta \varphi}{\Delta \gamma \cdot 2\pi}.$$

With $\beta = 0.7131$, $\gamma = 1.4279$, and $\lambda = 0.3724$ one finds that the drift should be 50 m or more and that \hat{V}_{eff} a bit less than 1.5 MV removes the energy spread. However, additional phase and energy spread develops during the drift because of the mutual repulsion of the beam particles.

Bunch Spreading in a 3D Envelope Calculation

A first order calculation of the bunch spreading along the 400 MeV transport has been made with TRACE-3D which accounts for the variations in longitudinal space charge force resulting from the changes in the transverse beam envelope using a linearized envelope equation. The result shown in Fig. 1 is based on the optics of the present 200 MeV line; both a 50 mA and a 0 mA solution are shown which minimize momentum spread and match booster lattice functions at the injection point. The debuncher is element 38 appearing along the axis of the envelope plot.

The data for the debunching calculation are summarized in Table I. The result, for the nominal initial conditions and the same 40m for debunching drift used with the present 201 MHz debuncher, is that the debuncher should provide $V_{\text{eff}} = E_0 T l = 1.54$ MV for 50 mA beam and 1.41 MV for $I = 0$. The drift distance is not especially critical. If it is too short a higher gradient is needed because the beam is not spread enough. Also the momentum spread will have somewhat more opportunity to grow in the rest of the transport. If the drift is too long the bunches span too much debuncher phase resulting in imperfect energy spread correction at the extremes.

Beam energy (kinetic)	401.46	MeV
Beam current averaged over pulse (\bar{I}_b)	50.	mA
Typical beam pulse length	2 - 22	μs
Bunch frequency of	201.25	MHz
Frequency of rf (f)	805.0	MHz
Repetition rate	15.0	Hz
H ⁻ /bunch	1.55	$\times 10^9$
Charge/bunch (q)	0.248	nC
Bunch area ($\sqrt{5}\sigma$)	8.17×10^{-5}	eVs
Normalized transverse emittance ($\sqrt{5}\sigma$)	6.88π	mm mrad
ΔE (FW)	2.546	MeV
$\Delta\varphi$ (FW)	11.8	deg

Table I: Properties of the 400 MeV Linac Beam

RF Structure

The 400 MeV transport design assumes a 2 cm radius minimum aperture at the debuncher. Table II gives the expected electrical properties of 400 MeV SCS with this bore.^[1] The shunt impedance and Q have been reduced from the SUPERFISH result by a conventional 15%. A 50 kW TV klystron has been chosen as a suitable rf generator providing 200

kW in pulsed service. The length of structure follows from the available power:

$$L_{\text{struc}} > \frac{V_{\text{eff}}^2}{P_{\text{max}} Z T^2} = 0.283 \text{ m} .$$

This is longer than $\beta\lambda$, so more than two cells are required. For three cells

$$P = \frac{(E_o T)^2}{Z T^2} L_{\text{struc}} = 143 \text{ kW} .$$

Cell length ($\beta\lambda/2$)	0.1329 m
Cavity bore radius (r_b)	2.0 cm
Effective shunt impedance (ZT^2)	41.4 M Ω /m
Transit time factor (T)	0.831
Quality factor (Q)	2.352×10^4
Filling time (τ_{fill})	9.3 μ s
R/Q characteristic ratio	117.0 Ω (true)

Table II: Electrical Properties of a 400 MeV SCS Cell at 8.05 MHz

Ideal debunching requires that the cavity phase be -90° at the bunch centers. As the passing bunches excite the cavity they produce a transient decelerating field which adds to the applied field to shift the phase progressively more negative. The induced voltage can be estimated by equating it to the voltage produced by the bunch charge appearing across the gap capacity. At resonance the stored energy is twice the time average of either the capacitive or inductive stored energy:

$$W = \bar{W}_{\text{cap}} + \bar{W}_{\text{ind}} = \frac{1}{4} C \hat{V}^2 + \frac{1}{4} L \hat{I}^2 = \frac{1}{2} C \hat{V}^2$$

where over-scored quantities are time averaged and the circumflexed quantities are peak values. Thus, for one cell one finds from Table II

$$C = \frac{2W}{\hat{V}^2} = \frac{2 \times 0.010135}{(0.1329 \times 10^6)^2} = 1.15 \text{ pF} .$$

Therefore, if one assumes all of the electrical energy is stored in the gap region, each bunch of 0.248 nC will generate a quadrature voltage of $V_{\text{beam}} = q/C = 216 \text{ V}$ on each gap. In an extreme impulse approximation that the entire beam pulse is short compared to cavity fill time the beam induced voltage would be over 2 MV. The proper phasor sum can be calculated if one knows the the time dependence of the 805 MHz fourier amplitude of the beam current.

Calculation of Cavity Excitation and Debuncher Performance

It is possible to proceed analytically, but it will be desirable to make a detailed calculation of the effect of the chosen beam loading compensation scheme. With this eventuality in mind and the necessary computer code already written,^[2] the calculations have been carried out with a time domain simulation of the beam-cavity interaction. Fig. 2 shows the quadrature voltage on the cavity as a function of time calculated by exciting an LRC cavity model with the beam current pulses produced by calculating the evolution of a nominal linac bunch in the linac-to-booster drift with space charge included. The ratio of average beam radius to beampipe radius was estimated from the envelope result shown in Fig. 1. The resulting bunch growth was similar. The effect of sum of this quadrature voltage and a fixed generator voltage on the debunching is plotted with the solid curves in the next two figures. Fig. 3 shows the time dependence of the mean bunch energy and Fig. 4 shows how the rms energy spread increases as the phase shifts so that the bunch arrives outside the most linear portion of the potential. The phase error after 3k bunches at 50 mA is 19° . Fig. 5 shows the superposition of an early and a late bunch. The dotted lines demark the the design tolerance of 0.1% FW on $\Delta p/p$.

Beam Loading Compensation

From these results one finds that beam loading degrades the debuncher performance substantially beyond the design tolerance. Because the cavity fill time of $9\ \mu\text{s}$ is the same as a typical beam pulse length, a system to control the cavity phase by feedback to the rf drive can not respond fast enough. However, the timing and intensity of linac beam batches are known rather well in advance. Introducing to the rf drive an appropriate level of quadrature drive just as the beam is to arrive will cancel the effects of the beam-induced voltage during most of the pulse. The rise time on the beam current due to chopper switching is $\sim 20 - 50\ \text{ns}$, whereas the klystron bandwidth is about 5 MHz. Therefore, the generator rf will be incorrect for $\sim 200\ \text{ns}$ or one tenth of a booster turn. This deficiency can be mitigated in two ways. First, the generator can be given an optimized head start, and, second, the structure can be chosen for lower R/Q than the SCS used for the linac. If the stored energy is greater, the beam makes a smaller perturbation of the cavity field. The DAW structure has higher stored energy because the basic mode is cognate to the TM02 mode of a pillbox cavity. The current associated with the extra magnetic energy flows mostly as displacement current in the disk-to-washer gap, so it does not correspondingly raise dissipation. Therefore, for this particular application DAW structure may be preferred. Because only three cells or so are required for the debuncher, the mode pattern does not have the complexity that causes concern about using the DAW in linacs. Table III gives the parameters of 400 MeV DAW with a 1.5 cm bore radius.^[3] The effect of increasing the bore from 1.5 to 2 cm should not be very serious; suppose for the sake of argument and comparison with the SCS of Table II one de-rates ZT^2 by 10%. The length of structure required to give $V_{\text{eff}} = 1.54\ \text{MV}$ at P_{max}

= 200 kW is

$$L_{\text{struc}} > \frac{V_{\text{eff}}^2}{P_{\text{max}} Z T^2} = \frac{(1.54 \times 10^6)^2}{0.2 \times 10^6 \times 43 \times 10^6} = 0.2757 \text{ m}$$

compared to $\beta\lambda = 0.2658 \text{ m}$. This is so close it would definitely be interesting to see if the larger bore really makes a 10% decrement in ZT^2 .

Cell length ($\beta\lambda/2$)	0.1329 m
Cavity bore radius (r_b)	1.5 cm
Effective shunt impedance (ZT^2)	48.7 M Ω /m
Transit time factor (T)	0.834
Quality factor (Q)	4.168×10^4
Filling time (τ_{fill})	16.5 μ s
R/Q characteristic ratio	77.6 Ω (true)

Table III: Electrical Properties of a 400 MeV DAW Cell at 8.05 MHz

The improvement resulting from using a two cell DAW structure is shown by the dotted curves in Figs. 2 and 3. The phase after 3k bunches has shifted by 11° . As shown in Fig. 6, the two cell DAW still requires some active compensation to keep the beam within the design $\Delta p/p$ window, but probably the booster would do fine without any feed-forward to the debuncher at routine operating intensity.

Note, however, that the Fig. 4 and 5 results do not include any variation in the linac output. Past operating experience indicates that there is some short-term fluctuation in the linac beam; a significant benefit of the debuncher is that it reduces the range of the bunch centroid fluctuation by the same ratio it reduces the spread within the bunch. However, to the calculated results for beam momentum spread some allowance for variation in the initial beam parameters should be added.

Conclusions/Recommendations

What has been discussed above can be easily summarized:

1. A debuncher is required, but ideal performance is not required.
2. The location of the present 201 MHz debuncher is quite suitable for a new 805 MHz debuncher.
3. A three-cell section of SCS dissipating about 145 kW provides the necessary 1.5 MV potential.
4. Compensation is needed for the beam loading of the debuncher.
5. The clear choice for the compensation technique is addition of a quadrature component to the klystron drive matched in time and magnitude to the anticipated beam batch.
6. The demands on the feed-forward scheme may be substantially reduced if it is practicable to implement the debuncher as a two-cell DAW structure within the chosen power constraint of 200 kW.

References

- [1] T. Jurgens, priv. comm., SUPERFISH calculation
- [2] S. Stahl and J. A. MacLachlan, "A User's Guide to ESME v. 7.1", Fermilab TM-1650 (26 Feb. 90), unpublished
- [3] A. Moretti, priv. comm., SUPERFISH calculation

8-JUN-90 14:31:21

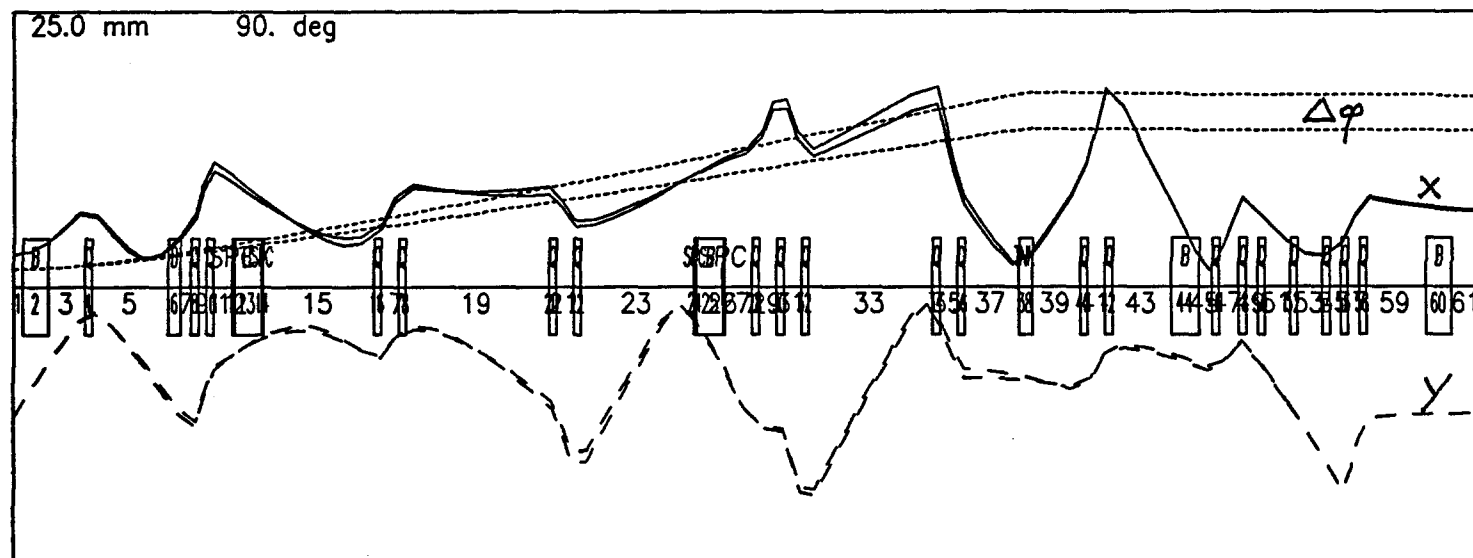
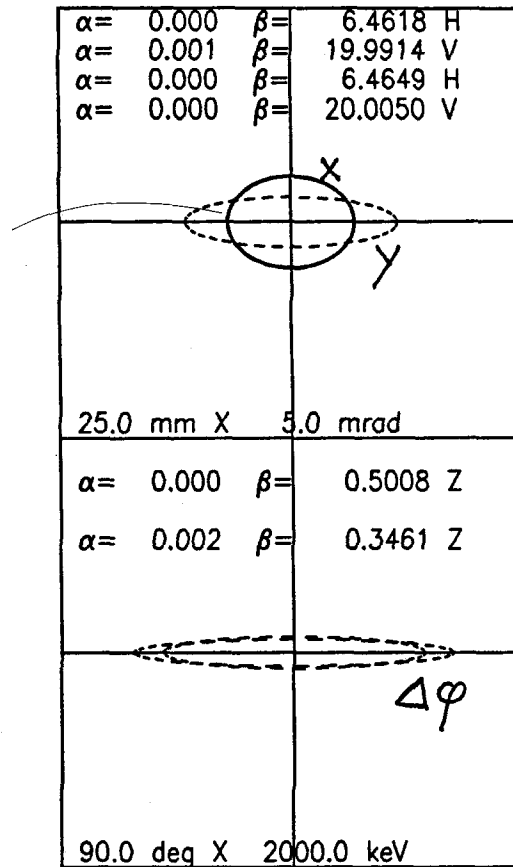
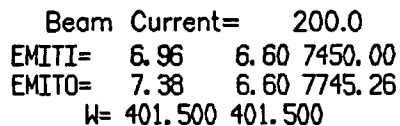


Figure 1: Beam envelope for the 400 MeV transport at $I_{\text{beam}} = 0$ and 50 mA

DEBUNCHER TRANSIENT R Volt 1 VS TIME

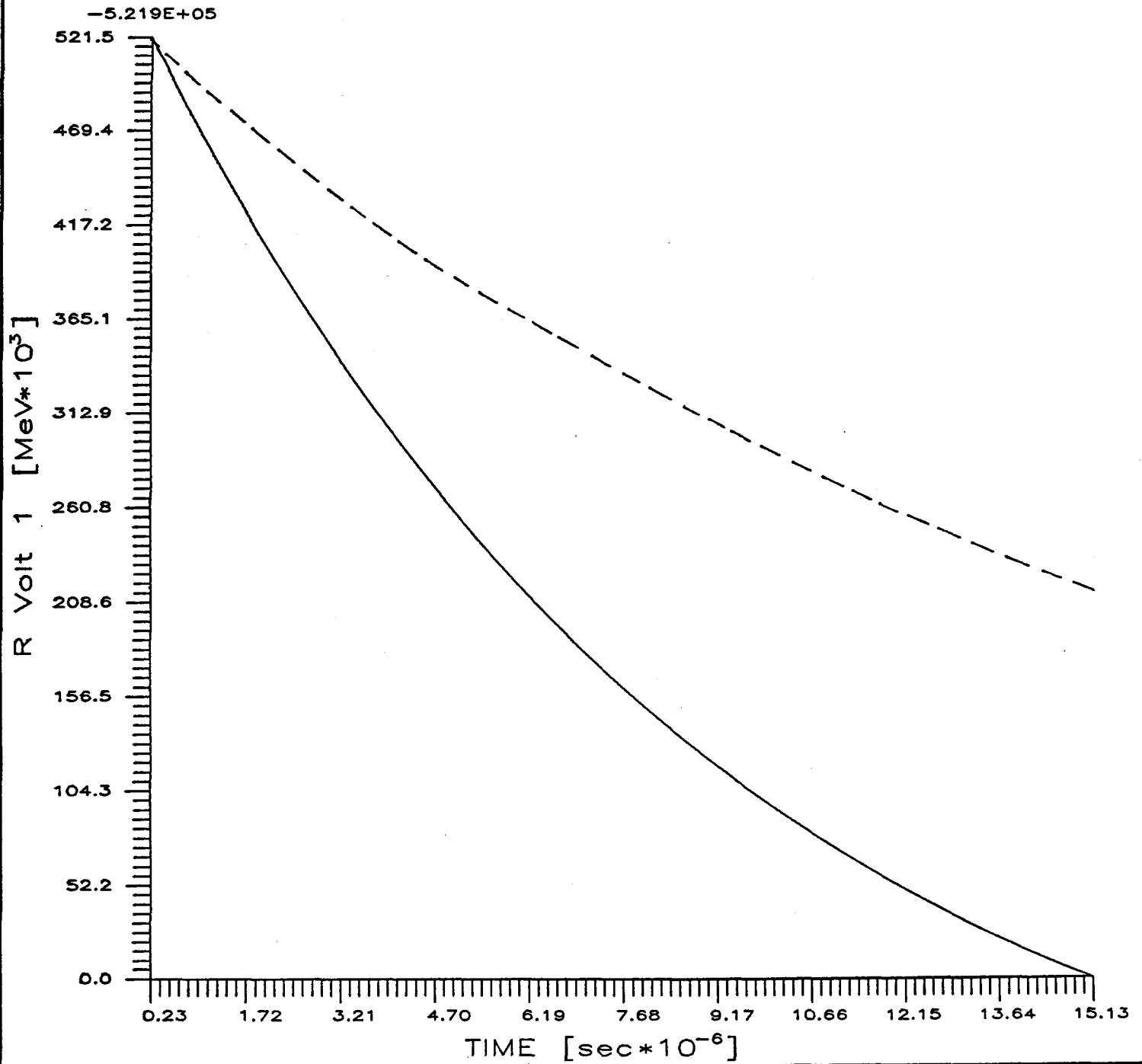


Figure 2: Decelerating voltage induced in the debuncher by 50 mA of beam for a three-cell SC debuncher (solid curve) and a two-cell DAW debuncher (dotted curve)

DEBUNCHER TRANSIENT EBAR VS. TIME

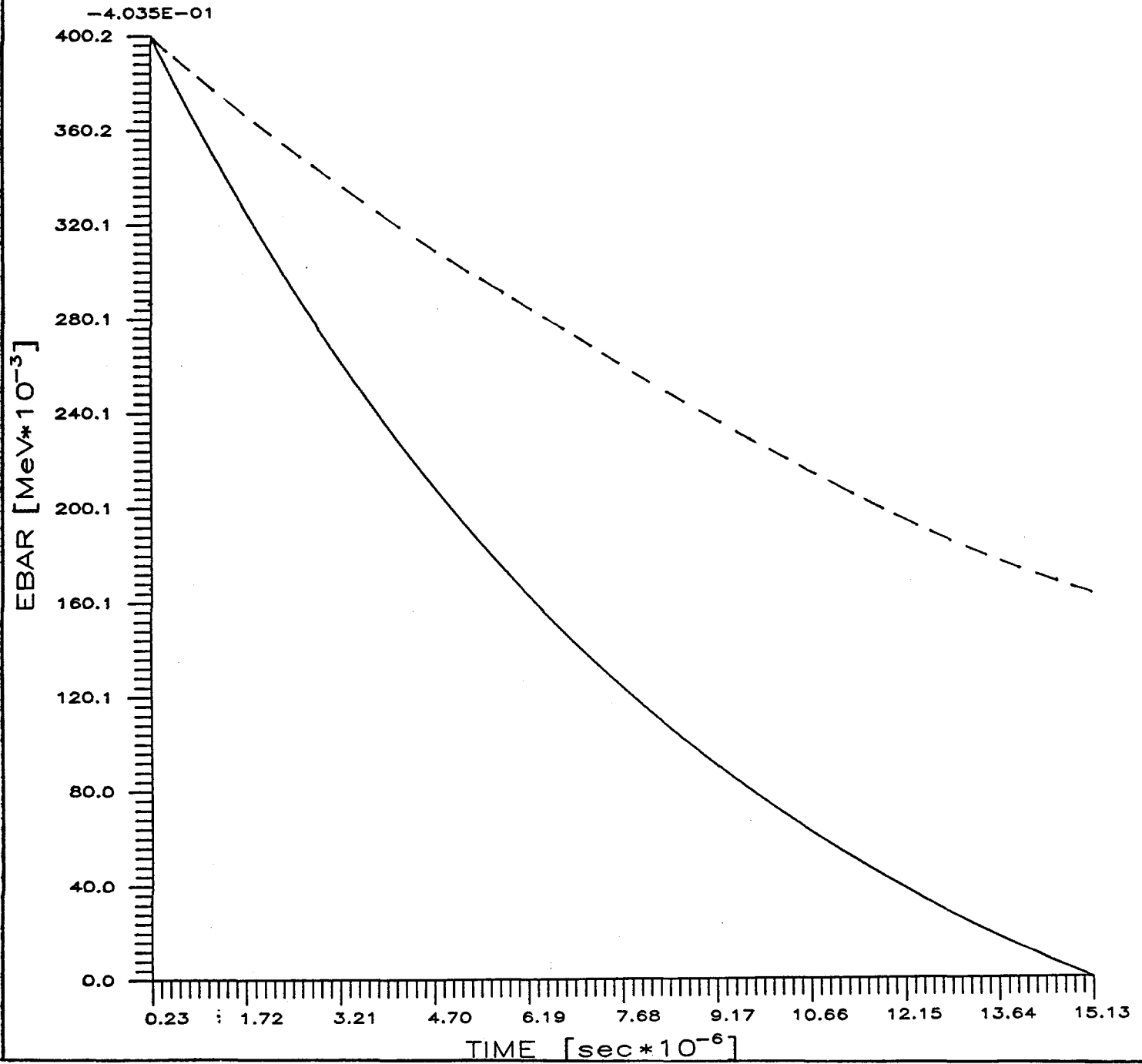


Figure 3: Mean bunch energy after debunching for a three-cell SC debuncher (solid curve) and a two-cell DAW debuncher (dotted curve)

DEBUNCHER TRANSIENT ERMS VS TIME

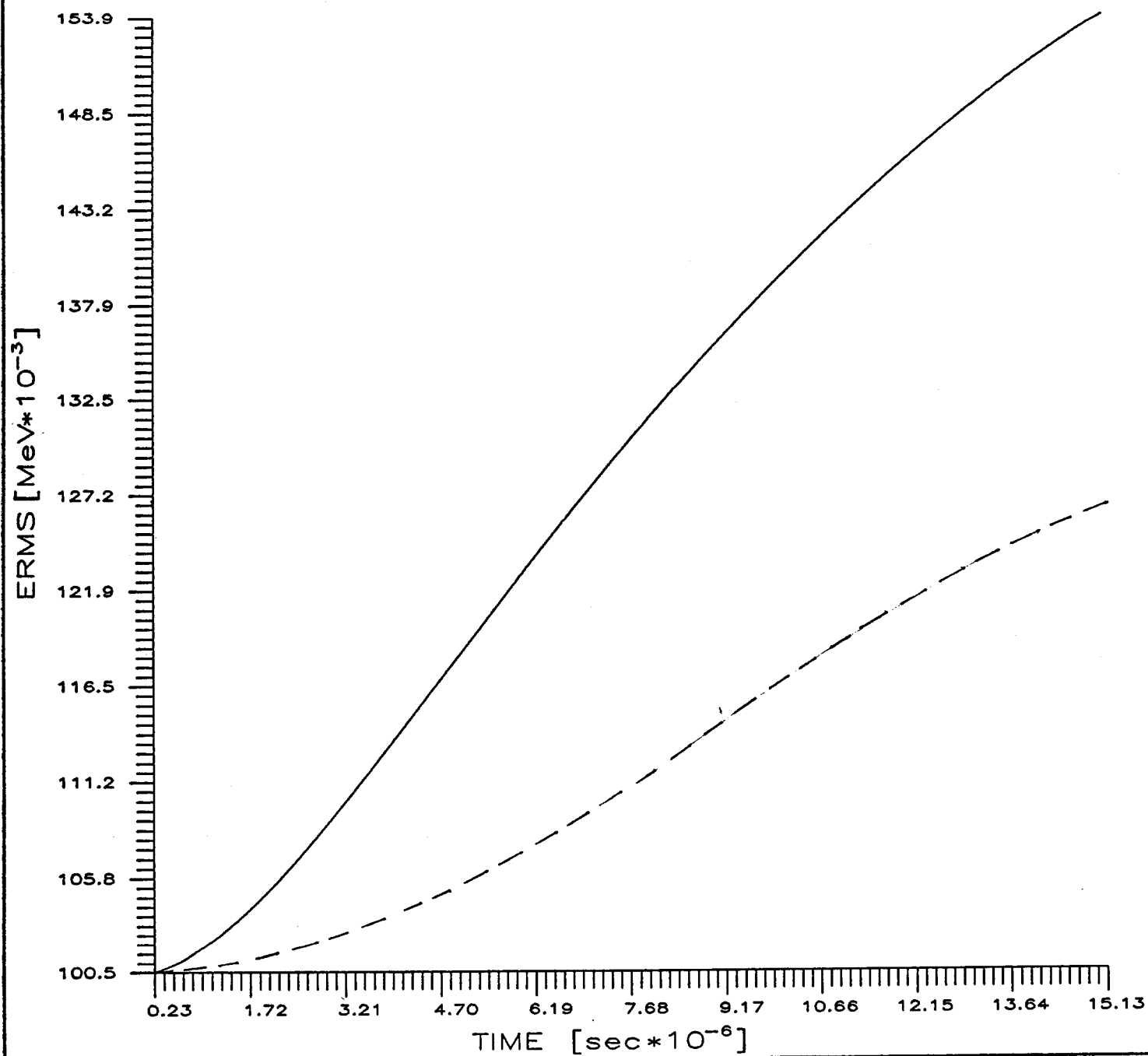


Figure 4: RMS spread of bunch energy after debunching for a three-cell SC debuncher (solid curve) and a two-cell DAW debuncher (dotted curve)

DEBUNCHER TRANSIENT TURN 3045 1.513E-05 SEC

H_s	S_s	E_s	h	V	ψ
1.8384E+01	2.9077E-02	1.3383E+03	4	1.534E+00	0.000E+00
ν_s	\dot{p}	η			
2.6561E-02	0.0000E+00	-4.9155E-01			

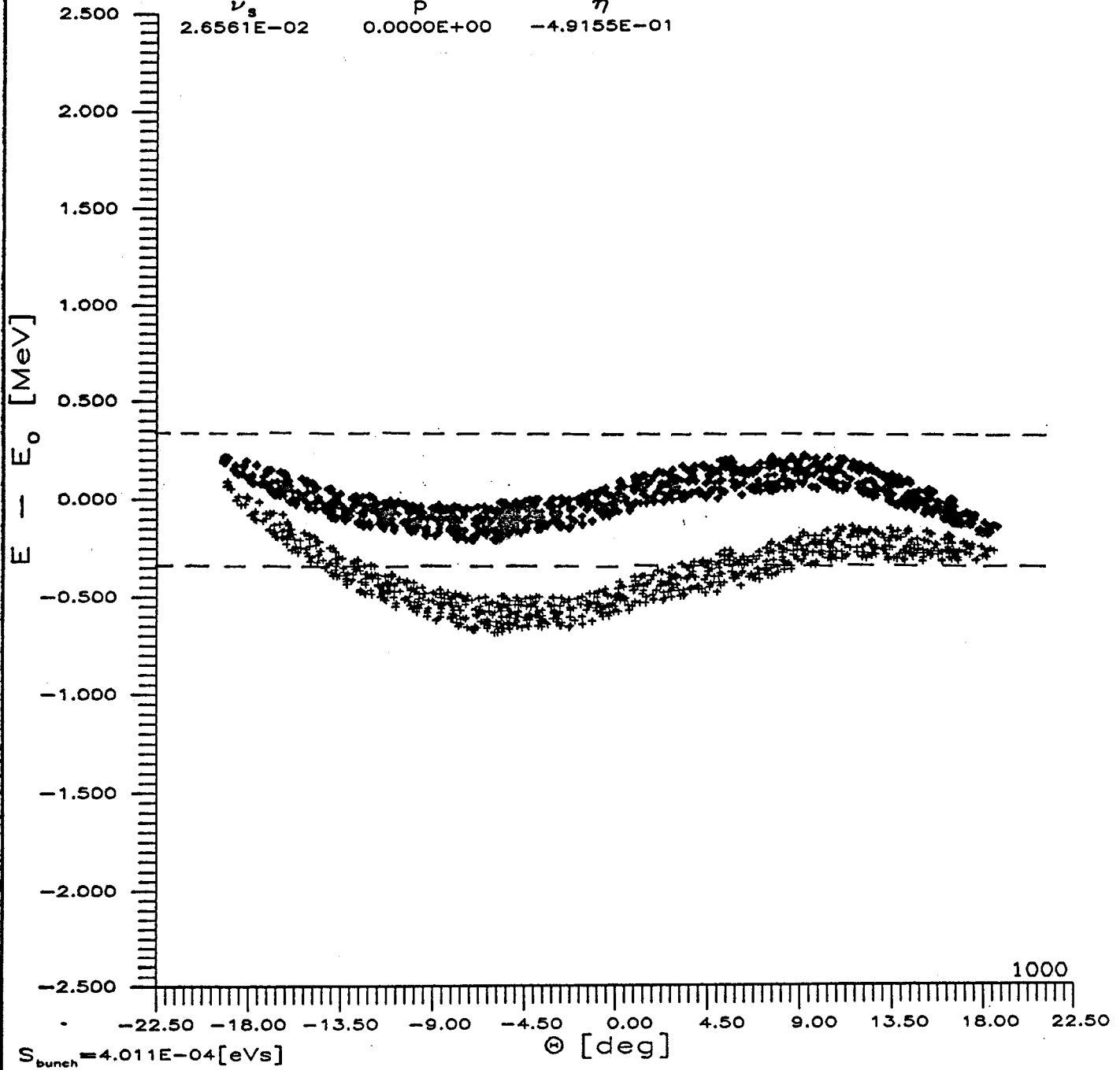


Figure 5: Comparison of initial bunch of debunched 50 mA beam with one 15 μ s later for a three-cell SC debuncher

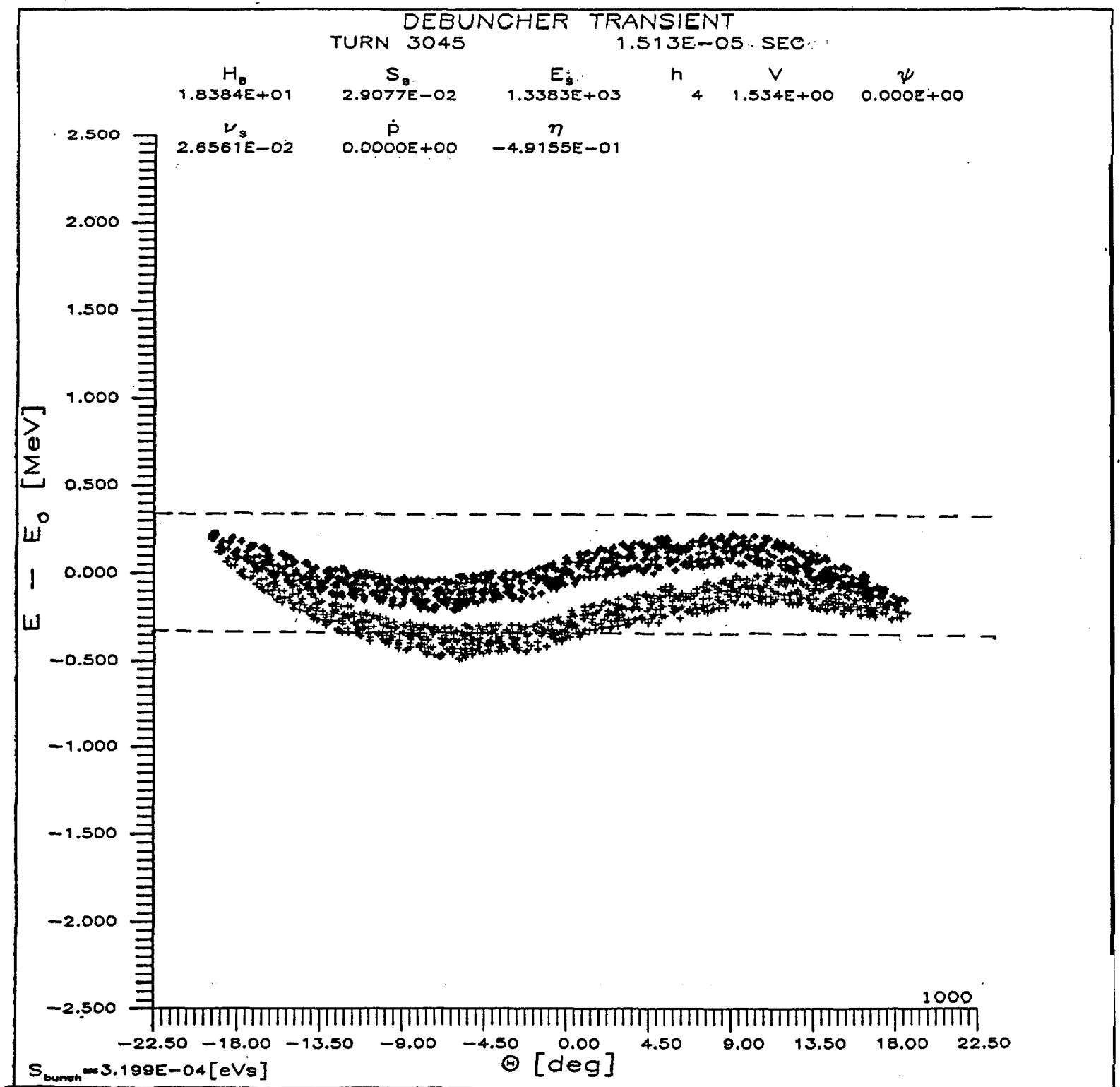


Figure 6: Comparison of initial bunch of debunched 50 mA beam with one 15 μs later for a two-cell DAW debuncher